Dendrochronologia 76 (2022) 126013

Contents lists available at ScienceDirect

Dendrochronologia

journal homepage: www.elsevier.com/locate/dendro

Growth phenological variations in the narrow-leaved ash (*Fraxinus angustifolia*) over the Mediterranean region: A simulation study☆

Filipe Campelo [a], Raúl Sánchez-Salguero [b,c], Patricia M. Rodríguez-González [d], Michele Colangelo [b,e], Ángela Sánchez-Miranda [c], Angelo Rita [e,f], Francesco Ripullone [e], J. Julio Camarero [b,*]

[a] Centre for Functional Ecology, Department of Life Sciences, University of Coimbra, Calçada Martim de Freitas, 3000-456 Coimbra, Portugal
[b] Instituto Pirenaico de Ecología (IPE-CSIC), Avda. Montañana 1005, E-50192 Zaragoza, Spain
[c] Departamento de Sistemas Físicos, Químicos y Naturales, Universidad Pablo de Olavide, 41013 Sevilla, Spain
[d] Forest Research Centre, School of Agriculture, University of Lisbon, Lisbon 1349-017, Portugal
[e] Scuola di Scienze Agrarie, Forestali, Alimentari e Ambientali, Università della Basilicata, Viale dell'Ateneo Lucano 10, 85100 Potenza, Italy
[f] Dipartimento di Agraria, Università degli Studi di Napoli Federico II, Via Università 100, 80055 Portici, Italy

ARTICLE INFO

Keywords:
Fraxinus angustifolia
Growing season
Vaganov-Shashkin model
Bimodal growth
Unimodal growth

ABSTRACT

Tree species inhabiting riparian forests under Mediterranean climate have evolved to face summer water shortage but may fail to cope with future increases in drought severity. Thus, understanding tree growth phenological variations in response to environmental conditions is necessary to assess the impact of seasonal drought in riparian forests. In this study, we investigated the response of stem radial growth to climate in the narrow-leaved ash (*Fraxinus angustifolia*) over its distribution in southern Europe. We simulated intra- and inter-annual growth patterns using the Vaganov-Shashkin (VS) model considering five sites subjected to summer drought but showing different climate conditions. The growth pattern in this species varied from unimodal in cool-wet sites to facultative bimodal in warm-dry sites. Bimodal patterns were characterized by two growth peaks coinciding with favorable climate conditions in spring and autumn. The spring growth peak occurs earlier (May) in warm-dry sites than in wet-cool sites (June–July). The variation in the season growth length and growth timing suggests different strategies adopted by this species to cope with summer drought. The VS model revealed different growth patterns across which would be relevant in predicting the response of this and other riparian tree species to climate warming and aridification. Differences in the length of the growing season, timings of growth peaks and the shift from unimodal to bimodal growth patterns should be considered when assessing growth adjustments to future climate scenarios.

1. Introduction

Climatic projections for the Mediterranean Basin predict increases in temperature and precipitation (Lelieveld et al., 2012), which are expected to have important impacts on forests due to shifts in tree growth phenology and growing season length (Peñuelas and Filella, 2001). While climate warming is expected to advance growth onset in Mediterranean tree species, higher temperatures would also rise evapotranspiration rates and intensify aridification shortening the effective growth period (Gordo and Sanz, 2010). In Mediterranean regions repeatedly exposed to seasonal summer drought, climate warming and increased drought have driven canopy dieback and growth decline in some riparian tree species, such as black alder (Valor et al., 2020), and common and narrow-leaved ash (Akilli et al., 2013; Enderle et al., 2019; Gomes Marques et al., 2018; Hauptman et al., 2016; Hultberg et al., 2020).

Trees can however adjust growth rates to changing environmental conditions, such as air and soil temperatures, day length, and soil water

☆ **Key message**: Intra-annual growth adjustments to climate in *Fraxinus angustifolia* are captured by process-based models.

* Corresponding author.
E-mail addresses: fcampelo@uc.pt (F. Campelo), rsanchez@upo.es (R. Sánchez-Salguero), patri@isa.ulisboa.pt (P.M. Rodríguez-González), michelecolangelo3@gmail.com (M. Colangelo), asanchezmirandam@gmail.com (Á. Sánchez-Miranda), angelo.rita@unibas.it (A. Rita), francesco.ripullone@unibas.it (F. Ripullone), jjcamarero@ipe.csic.es (J.J. Camarero).

https://doi.org/10.1016/j.dendro.2022.126013
Received 6 June 2022; Received in revised form 10 September 2022; Accepted 4 October 2022
Available online 7 October 2022

content (Vaganov et al., 2006). In seasonal arid regions, the ability to coordinate secondary growth with favorable environmental conditions and limit or even cease growth during unfavorable periods, such as the dry Mediterranean summer, is critical (Mitrakos, 1980). For instance, species-specific phenological responses are modulated by climate site conditions (e.g., temperature, soil water content), which determine species' capacity to face climate change (Chuine et al., 2000) and capture resources (Nord and Lynch, 2009). In cold-limited areas, warming-driven extended phenology may point to increased resource acquisition (Nord and Lynch, 2009), which can enhance tree growth (Begum et al., 2013; Sánchez-Salguero et al., 2018a; but see Etzold et al., 2022) and promotes range shifts (Nadal-Sala et al., 2019). Although extended growing seasons are expected at cold sites in response to climate warming, a similar phenological response remains questionable at mid-latitude, seasonally dry sites (Ziaco et al., 2018) such as Mediterranean regions. At these drought-prone sites, the potential benefit of a longer growing season due to warming may be compromised by an extended period of water shortage.

Mediterranean tree species usually have high capacity to adjust growth to current conditions, which is advantageous to face the double stress imposed by rainfall (dry summers) and temperature (cold winters, particularly in continental or mountain areas) seasonality (Mitrakos, 1980). As a result, cambial activity in several Mediterranean tree species follows a bimodal pattern to benefit from favorable conditions in spring and autumn (Camarero et al., 2010; Cherubini et al., 2003), which is responsible for the formation of intra-annual density fluctuations (Campelo et al., 2007, 2018). This bimodal growth pattern is species- and site-dependent, varying from facultative to mandatory, and depends on site climate conditions (Campelo et al., 2021; Pacheco et al., 2018). Therefore, in the Mediterranean Basin, where rainfall show high variability at the intra- and inter-annual scale (Serrano-Notivoli et al., 2018), the capacity of trees to adjust their growth rates to climate conditions, particularly soil water availability, is critical under a warming context (Garcia-Forner et al., 2019; Vieira et al., 2019).

Tree growth responses to climate have been poorly investigated in riparian tree species such as shallowly-rooted, water-spending (anisohydric) ash species whose growth often depends on shallow soil water sources (Köcher et al., 2009; Singer et al., 2013; Stella et al., 2013). Floodplain and riparian forests are also highly threatened by land conversion, hydrogeomorphological alterations such as dam building or gravel extraction leading to channel bed incision, which generally reduces water availability (e.g., Stella et al., 2013), and direct groundwater capture through drainage (e.g., Mikac et al., 2018). Therefore, severe and prolonged droughts might change hydrological regimes (e.g., descending groundwater levels) making these forests more vulnerable to further aridification triggering drought-induced dieback (Skiadaresis et al., 2019). On the other hand, it could be expected that higher soil water availability in Mediterranean riparian and floodplain forests could buffer them against drought impacts because trees could access groundwater and precipitation-derived soil moisture (Heklau et al., 2019; Camarero et al., 2021a, 2021b).

In the Mediterranean basin, the narrow-leaved ash (*Fraxinus angustifolia* Vahl) is the main ash species with a relatively large geographical distribution and ecological amplitude, extending from riparian areas with permanent water availability to floodplains with occasional floods (Gomes Marques et al., 2018). Because precipitation is the primary source of vadose zone soil moisture it is expected that the *F. angustifolia* growth is linked to variables reflecting soil water availability (e.g., precipitation, drought severity; cf. Camarero et al., 2021a, 2021b; Rodríguez-González et al., 2021). In addition to the ash's sensitivity to low summer precipitation, habitat changes may explain its current endangered status in regulated basins, which favors its replacement by other tree species better adapted to thrive in closed stands (Janík et al., 2016; Trlin et al., 2021). Here we argue that narrow-leaved ash trees adjust their growth pattern and growing season length to prevailing climatic conditions (cf. Sánchez-Salguero and Camarero, 2020), minimizing exposure to summer drought stress while maximizing carbon assimilation (Chuine, 2010; Saderi et al., 2019). For this reason, understanding the intra-annual growth dynamics of this species would allow improving the management and conservation of threatened Mediterranean riparian ecosystems (Stella et al., 2013). The information gathered from process-based growth models and growth responses to climate can be used to forecast the responses to climate of Mediterranean riparian forests (e.g., Sánchez-Salguero et al., 2018b).

Here we investigate how narrow-leaved ash (hereafter referred to as ash) adjusts stem radial growth to climatic conditions at five sites along a geographic gradient in precipitation and temperature. We use tree-ring width data to fit the process-based Vaganov-Shashkin (VS) growth model to: (i) assess radial growth responses to climate, (ii) evaluate the relative importance of temperature, precipitation and soil water content as drivers of radial growth, and (iii) investigate how intra-annual growth patterns respond to climate across ash populations. We expect that this species may shift the intra-annual growth pattern from unimodal, with a growth peak around the summer solstice, in continental, cold-wet sites to bimodal in coastal, warm-dry sites. We also expect a shorter growing season in cold-wet sites and a longer growing season in warm-dry sites.

2. Material and methods

2.1. Study sites and tree species

The five sites selected for this study cover contrasting environmental conditions across the ash distribution area (Table 1). Three sites were in Spain, one in southern Portugal and another one in northern Italy (Fig. 1). The two driest-warmest sites are located on the south-western coast of the Iberian Peninsula: the Odelouca (ODE) site is located on the Odelouca river (southern Portugal) and the Doñana (DON) site is located in the Doñana floodplain forest (southwestern Spain). The other sites in Spain are two sites situated in the Ebro basin: Soto de la Remonta (near Tudela – TUD– and Nieva de Cameros, La Rioja – NdC). The last site (Ticino, TIC) is located in the "Parco Lombardo della Valle del Ticino" (Lonate-Pozzolo basin) within the Ticino Valley Natural Park (Northwest Italy). The Iberian sites have negative annual water balances, whereas the Italian site has a positive water balance. The sites are dominated by ash which is a non-phreatophytic, hydrophilic, moderately thermophilic and heliophilous species, with shallow roots that usually do not penetrate gravel substrates and use mainly vadose zone water to maintain tree growth, making it very sensitive to fluctuations in soil moisture (Camarero et al., 2021a, 2021b). For detailed information on stand structure and climatic conditions at the five study sites see the Supplementary material (Methods S1).

2.2. Climate data

Due to the lack of long-term, homogeneous local climate data in the study sites, the CRU TS ver. 4.04 gridded database was used (Harris et al., 2014). For each site, we downloaded long-term series of mean temperature and precipitation corresponding to the nearest 0.5° grid point, using the Climate Explorer webpage (https://climexp.knmi.nl). The gridded data were used to calculate monthly water balance as the difference between precipitation and potential evapotranspiration (P-PET), which was estimated using a modified Thornthwaite method.

2.3. Field sampling and dendrochronological data

We selected from 6 to 17 mature and dominant trees per site (Table 2). For each tree the diameter was measured at breast height (Dbh), i.e. at 1.3 m, and two increment cores were sampled using 5-mm Pressler increment borers. Cores were air dried, mounted on wooden supports and carefully sanded. Tree rings were visually cross-dated and tree-ring widths were measured to the nearest 0.01 mm using a stereomicroscope and the LINTAB measuring table device connected to a

Table 1
Location of the study sites. Mean annual temperature (MAT), total annual precipitation (P), potential evapotranspiration (PET), annual and summer (JJA, June to August) water balance (P-PET) is given for the period 1970–2009, data from the closest grid-point (CRU TS4.04).

Site		Latitude (N)	Longitude (W/E)	Elevation (m)	MAT (°C)	P (mm)	PET (mm)	P-PET$_{annual}$ (mm)	P-PET$_{JJA}$ (mm)
Doñana	DON	37°06'	6°39' W	69	18.2	525.3	1344.1	-818.8	-544.5
Odelouca	ODE	37°14'	8°30' W	120	16.6	617.5	1093.1	-475.5	-428.3
Nieva de Cameros	NdC	42°13'	2°40' W	980	9.13	734.5	940.3	-205.8	-303.8
Tudela	TUD	42°07'	1°35' W	257	14.2	543.3	1118.5	-575.2	-396.5
Ticino	TIC	45°26'	8°50' E	202	12.8	1104.2	776.7	327.5	-113.1

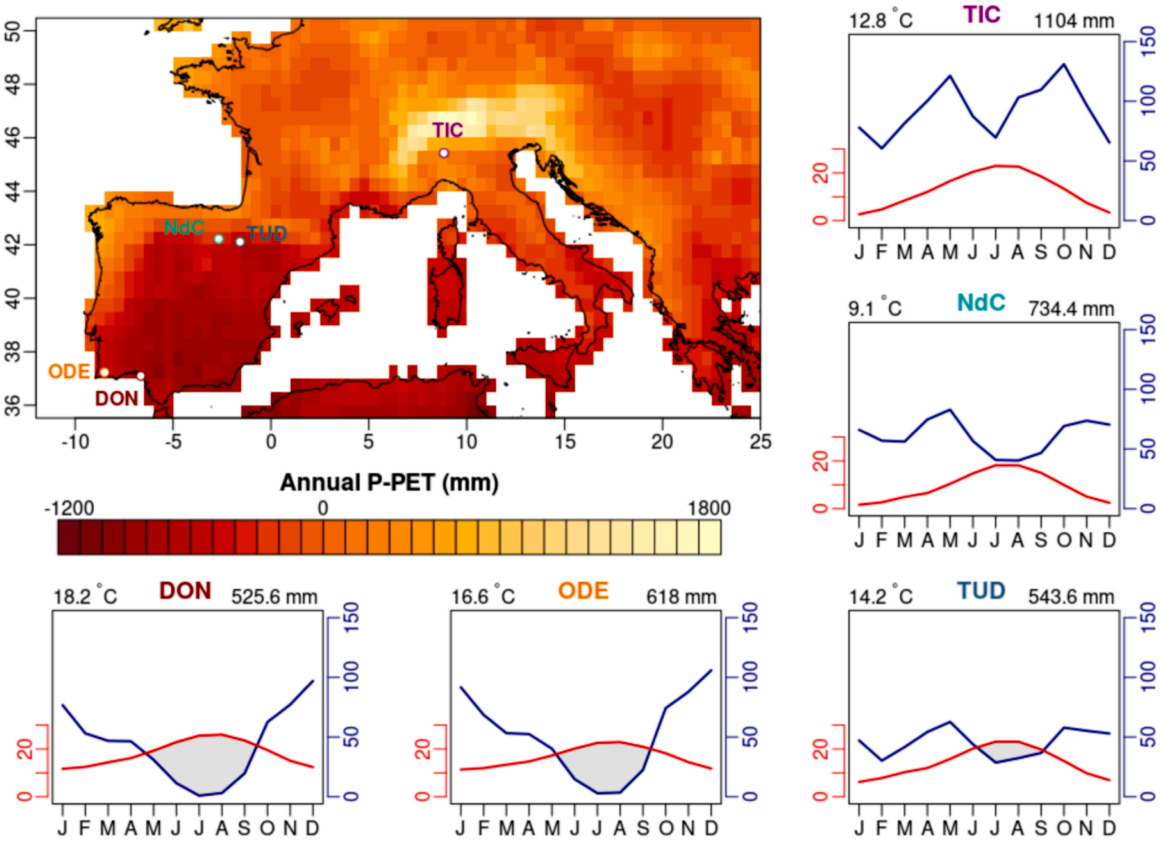

Fig. 1. Location of the five study sites across southern Europe; the color scale shows annual water balance calculated as precipitation (P) minus potential evapotranspiration (PET). Climatic diagrams of the studied sites for the period 1970–2009 based on data downloaded from the Climatic Research Unit (CRU TS4.04). Site abbreviations: DON, Doñana; NdC, Nieva de Cameros; ODE, Odelouca; TIC, Ticino; TUD, Tudela.

Table 2
Number of trees and dendrochronological statistics of *Fraxinus angustifolia* populations at studied sites. Abbreviations: Dbh, diameter at breast height; TRW, tree-ring width; AR1, first-order autocorrelation; Ms, mean sensitivity, Rbar, mean inter-series correlation; EPS, Expressed Population Signal. The Rbar and the EPS values were calculated using residual-series for the best-replicated period (1970–2009).

Site	No. trees (cores)	Dbh (cm)	Age at 1.3 m (years)	TRW (mm)	AR1	MS	Rbar	EPS	Period (EPS > 0.85)
DON	12 (23)	30.0 ± 1.2	61 ± 12	2.18 ± 0.41	0.71	0.31	0.36	0.87	1947–2014
ODE	12 (24)	46.0 ± 3.0	62 ± 13	3.97 ± 0.91	0.62	0.37	0.32	0.83	1953–2009
NdC	6 (12)	31.9 ± 1.9	45 ± 13	2.32 ± 0.53	0.67	0.27	0.65	0.94	1963–2015
TUD	17 (26)	31.0 ± 2.0	47 ± 12	2.77 ± 0.43	0.63	0.33	0.26	0.86	1970–2016
TIC	16 (23)	36.0 ± 1.4	59 ± 14	3.21 ± 0.74	0.66	0.27	0.21	0.80	1969–2017

computer with the TSAP-Win (Time Series Analysis Program) software (Rinntech, Heidelberg, Germany). Cross-dating quality of tree-ring series was evaluated using the COFECHA program (Holmes, 1983). Cambial age at 1.3 m was given by the maximum number of rings when the pith was present and the curvature of the innermost rings was used to estimate pith offset when the pith was absent in the core.

To remove age-related growth trends and competition effects, a one-step detrending was applied to each tree-ring width series, using the packages dplR (Bunn, 2008) and detrendeR (Campelo et al., 2012) for the R program (R Development Core Team, 2021). Cubic smoothing splines with 50% frequency-response cutoff equal to 2/3 of the individual series length were applied to remove low- to medium-frequency signals and enhance the year-to-year variations. Then, the first-order autocorrelation was removed by fitting autoregressive models. Finally, ring-width chronologies were obtained for each site by averaging residual series using a bi-weight robust estimate of the mean to reduce

outliers' effect. The statistical quality of each chronology was evaluated using the following variables: first-order autocorrelation (AR1), mean sensitivity (MS), mean correlation between series (Rbar) and Expressed Population Signal (EPS) (Fritts, 1976). The EPS defines how well the developed chronologies represent a theoretical, infinitely replicated chronology (Wigley et al., 1984). Following these authors, we used a threshold of EPS > 0.85 to determine the best-replicated period for each chronology and to define the reliable common-period for all chronologies. Mean tree-ring width, MS and AR1 were calculated on raw data, whereas indexed-series were used to compute Rbar and EPS (Table 2).

For each site, the residual ring-width (TRW_i) chronology was used to investigate the climatic signal and calibrate the VS model. For the common period (1970–2009), Pearson correlations coefficients were calculated between monthly climatic variables (mean air temperature, precipitation, soil water content) and TRW_i chronologies for each site (Table 3).

2.4. Vaganov-Shashkin process-based model of tree-growth

The VS model was used to simulate TRW_i as a function of daily temperature (T) and precipitation (P), based on the principle of limiting factors (Evans et al., 2006; Vaganov et al., 2006). For each site, the daily precipitation sums and mean daily temperatures were extracted from the E-OBS gridded (0.1° spatial resolution) climate dataset (v25.0e; Cornes et al., 2018). The VS model was calibrated by tuning 10 parameters (Table S1) using a simple optimization algorithm for the period 1970–2009. Due to the short best-replicated common period (n = 40) to all sites, no validation procedure on independent data was performed. To avoid model over-fitting, a restricted and realistic range of values for each parameter was defined (Table S1). To ensure that all models were tuned under the same conditions, both the random seed (999) and the initial values were the same for all models. In addition, each parameter was optimized one after the other, while the remaining parameters were kept constant at their previous optimized values. In doing so, all parameters were tuned automatically.

Lastly, phenological growth events including the dates of growth onset, growth peak and growth cessation (presented as DOY, day of the year) were derived from daily growth rates simulated by the VS model.

2.5. Statistical analyses

A Principal components analysis (PCA) was applied to the covariance matrix of residual chronologies to evaluate the shared variance among chronologies for the period 1970–2009 to detect growth and spatial patterns. The PCA was performed by singular value decomposition, using the R function prcomp after standardizing variables to have mean zero and standard deviation one. In the principal component graph (biplot), site representation was based on the magnitude of the correlation (loadings) between sites and the given principal component. The scores of the three first PCs were used to estimate spatial Pearson correlations ($p < 0.05$) with soil water content.

To assess climate-growth associations, Pearson correlations were calculated by relating ring-width indices (residual chronologies) with monthly and seasonal climatic variables (mean air temperature, precipitation, and soil water content) from previous October to September of the year of tree-ring formation. Both the PCA and the correlations were calculated for the period 1970–2009.

3. Results

3.1. Tree-ring width and climate data

Well-replicated tree-ring width chronologies were produced in the five study sites (Table 2). The shortest and longest chronologies were 57 years and 96 years long in the coldest site (NdC) and in the wettest site (TIC), respectively. The widest tree-rings were found in the dry-warm ODE site (3.97 mm yr^{-1}), while the narrowest rings were found in the driest DON site (2.18 mm yr^{-1}). Growth rates in TUD (2.77 mm yr^{-1}) and TIC (3.21 mm yr^{-1}) sites showed similar values, whereas the coldest NdC site showed low growth rates (2.32 mm yr^{-1}). The highest value of AR1 was found in the DON site, whereas the lowest was found in the ODE site (Table 2). In this site, MS reached the maximum value, while lower MS values were found in NdC and TIC. The best-replicated common period (1970–2009) was defined by EPS > 0.85 (Table 2 and Fig. 2). For the period 1970–2009, the Rbar and EPS values peaked in DON and NdC sites, while the lowest values were found in the wet TIC site.

3.2. Local climate-growth responses

Only TIC and TUD sites showed positive correlations between growth and precipitation in summer (June and August in TUD and July in TIC). Tree-ring width chronologies were positively correlated to February temperature in the DON and ODE sites, which suggests that warmer conditions could advance growth onset (Table 3). A negative correlation was found between growth rates and temperature in June (July) in TIC (TUD). In TIC, growth correlated directly with July precipitation. In DON and ODE, growth showed a positive correlation with April—May soil water content (Table 3), whereas in the other sites the highest correlations with soil water content were found in July (in TIC) and June and August (NdC and TUD).

Table 3
Pearson's correlation coefficients between residual chronologies and monthly climatic data (TMP, mean temperature; PRE, total precipitation; and SWC, soil water content) for the best-replicated period 1970–2009. Values in bold indicate significant correlations at $p < 0.05$. Site abbreviations: DON, Doñana; NdC, Nieva de Cameros; ODE, Odelouca; TIC, Ticino; TUD, Tudela.

Variable	Site	oct	nov	dec	JAN	FEB	MAR	APR	MAY	JUN	JUL	AUG	SEP	oct-SEP	APR-MAY	JUL-AUG
TMP	DON	-0.01	-0.04	0.22	0.21	**0.37**	0.15	-0.11	-0.17	0.10	0.08	0.01	0.30	0.20	-0.19	0.05
	ODE	0.21	0.13	**0.49**	**0.32**	**0.43**	0.20	0.02	-0.04	0.09	-0.01	0.01	0.25	**0.36**	-0.02	0.00
	NdC	**-0.44**	0.31	0.11	-0.06	-0.06	-0.15	0.08	-0.24	-0.18	-0.13	0.01	0.07	-0.09	-0.13	-0.07
	TUD	-0.14	0.05	0.01	0.04	0.23	-0.11	0.09	-0.16	-0.21	**-0.33**	-0.06	-0.09	-0.13	-0.06	-0.23
	TIC	0.02	-0.07	0.03	-0.26	-0.13	-0.07	0.08	-0.03	**-0.33**	-0.22	-0.03	0.07	-0.18	0.02	-0.16
PRE	DON	0.09	0.30	0.17	0.21	0.19	-0.03	0.28	0.22	-0.08	-0.19	-0.28	0.04	**0.47**	**0.34**	-0.28
	ODE	0.12	**0.33**	**0.39**	0.25	0.25	-0.10	**0.37**	0.14	-0.12	0.10	-0.22	0.02	**0.58**	**0.36**	-0.08
	NdC	**0.38**	0.14	0.17	-0.02	-0.15	-0.10	0.04	0.22	0.20	0.21	0.22	-0.14	**0.41**	0.18	0.27
	TUD	0.01	0.31	0.00	0.18	-0.14	0.00	0.03	0.28	**0.35**	0.08	**0.33**	0.02	**0.46**	0.22	0.25
	TIC	0.23	0.04	**-0.34**	0.18	0.06	0.12	0.14	0.22	0.25	**0.37**	-0.02	-0.26	0.29	0.28	0.18
SWC	DON	0.12	0.31	0.31	**0.34**	**0.42**	**0.39**	**0.51**	**0.54**	**0.44**	**0.42**	**0.37**	0.30	**0.47**	**0.54**	**0.40**
	ODE	0.11	**0.33**	**0.46**	**0.47**	**0.49**	**0.42**	**0.58**	**0.57**	**0.47**	**0.45**	**0.43**	**0.41**	**0.56**	**0.59**	**0.44**
	NdC	**0.41**	**0.40**	**0.45**	0.28	**0.32**	0.26	0.24	**0.32**	**0.35**	**0.36**	**0.41**	0.26	**0.50**	0.30	**0.40**
	TUD	**0.34**	**0.46**	**0.36**	**0.38**	0.29	0.26	0.25	**0.38**	**0.50**	**0.43**	**0.51**	**0.51**	**0.55**	**0.34**	**0.49**
	TIC	0.06	0.03	-0.11	0.02	0.04	0.11	0.19	0.26	**0.35**	**0.55**	0.26	-0.06	0.20	0.26	**0.42**

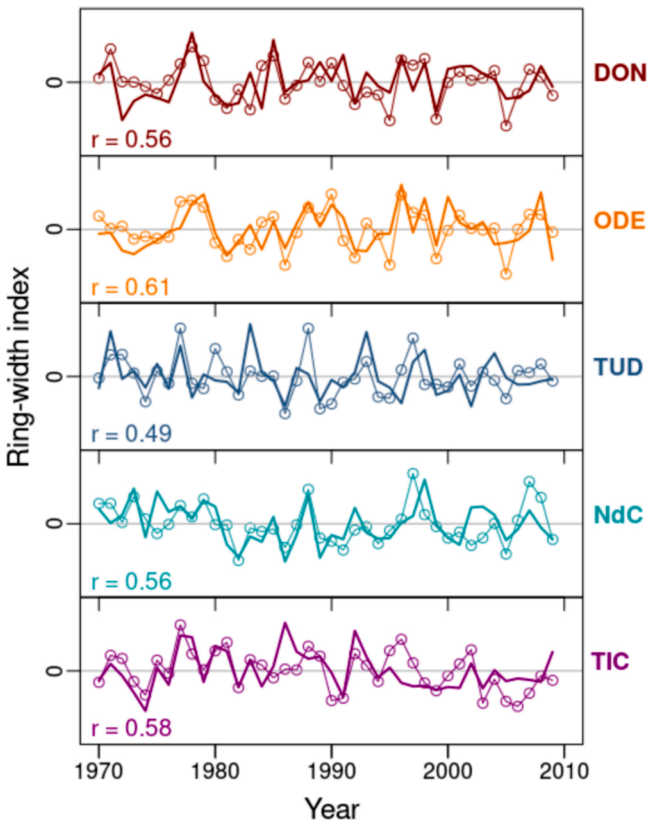

Fig. 2. Observed (thick lines) versus Vaganov-Shashkin simulated (thin lines) ash ring-width chronologies considering the best-replicated common period (1970–2009). The Pearson correlation coefficients (r) between observed and simulated chronologies are given for each site and are significant ($p < 0.05$) in all cases.

3.3. Regional climate—growth responses

The PCA biplot of the first two principal components (PCs), which accounted for 60.1 % of the common variance in growth rates, allowed disentangling relationships among sites (Fig. 3). The first three PCs of the PCA accounted for 81.3 % of the shared growth variance. Chronologies from DON and ODE loaded positively on the first PCA axis (PC1) (Fig. 3 and Table S2), whereas NdC and TUD loaded negatively on the second PCA axis (PC2). The TIC chronology loaded positively on the third PCA axis (PC3). Chronologies from south-western Iberia (DON and ODE) were highly correlated ($r = 0.73$, $p < 0.001$), whereas north-eastern chronologies (NdC and TUC) showed no significant correlation ($r = 0.25$, $p = 0.11$).

The dependence of ash growth on soil water content is evident in the spatial correlations for the first three PCs derived from ring-width chronologies (Fig. 4), reflecting the importance of soil water content over the growing season to determine growth variations (Table 3). A strong positive correlation was found between soil water content and the PC1 scores (Fig. 4), whereas PC2 scores (inverted values) showed high positive correlations with July soil water content in north-eastern Iberia. Finally, the third principal component (PC3) showed positive correlations with April–June soil water content in northern Italy (TIC site).

3.4. VS model: intra-seasonal growth patterns

Positive correlations between observed and VS simulated chronologies were found in all sites confirming the robustness of fits (Table 4). The highest correlations were found in ODE ($r = 0.61$) and TIC ($r = 0.58$). Differences in the intra-annual growth pattern estimated by the VS model were caused by differences in the limiting climatic factors of growth among sites (Fig. 5). In all studied sites, the VS model simulations were in agreement with the correlations obtained between ring-width chronologies and climatic variables (Table 3). In DON and ODE sites, the main limiting factor was soil water content along the growing season (Fig. 5), while in TUD the limiting factor changed over the growing season, with low temperatures being limiting in winter and low soil water content in the other months. In NdC and TIC sites, tree growth was limited by coldness during the start and end of the growing season (Fig. 5). The intra-annual growth pattern predicted by the VS model shows geographic variation, being unimodal at the TUD and NdC sites, whereas at the dry-warm DON and ODE sites a facultative bimodal growth pattern appeared (Figs. 6 and 7). In the wet-cool TIC site a tendency towards a second growth peak in late summer was observed.

The length of the growing season and the existence of a summer quiescent period showed also great variation among sites. At the DON and ODE sites, the growing season was longer and presented a summer stop, whereas in the other sites the growing season was shorter and high growth rates could occur during the summer. Short growing seasons were predicted by the VS model for cold sites (NdC and TIC), with the site at the highest altitude (NdC) showing the shortest growing season (Fig. 6). The short-duration of the growing season in NdC and TIC was associated with a unimodal growth pattern without a summer quiescent period (Fig. 7).

3.5. VS model: phenological growth events

The timing of growth onset ranged from middle February (DOY ~ 50) to late April (DOY ~ 110). The dry-warm DON and ODE sites started to grow earlier than the other sites, while the coldest NdC site was the last to start to growth (Fig. 6). The wet TIC site showed low intra-site variation in terms of the timing of growth onset. The timing of maximum growth showed high inter-site variability, ranging from early May (DOY ~ 130) to late June (DOY ~ 180) and the intra-site variability was low in the NdC site (Fig. 6). Considering growth cessation dates, the DON and ODE sites showed high variability, probably linked to their bimodal growth patterns. Low variability was observed for growth cessation in NdC and TIC sites.

4. Discussion

Our results demonstrated that *F. angustifolia* populations adjusted their radial growth phenology to site climate conditions, including features such as growing season length, intra-seasonal growth patterns, and the time when the growth rates are highest. These findings support our first hypothesis that this species maximizes tree growth by adjusting the intra-annual growth pattern to local climate conditions. As expected, longer growing seasons with bimodal growth patterns were predicted for dry-warm coastal sites, whereas in inland wet-cold sites the growing season was shorter and growth followed a unimodal pattern. In the wet-cool TIC site a slightly bimodal pattern was found, but without summer stop. This work shows that the VS model and similar process-based models can be applied to assess tree growth responses under different climate conditions.

4.1. Climate-growth responses: the importance of soil moisture

Tree growth in ash was very coupled to climate conditions during the growing season, in particular to soil water content, which revealed differences between sites (Fig. S1). In fact, the highest correlations were obtained between monthly soil water content and growth (Table 3), as expected for non-phreatophyte species. At the dry-warm DON and ODE sites, positive correlations between February temperatures and chronologies suggested that growth onset could be anticipated by warmer conditions (Begum et al., 2018), which agree with phenological observations in *F. excelsior* (Roberts et al., 2015), with leaf unfolding advancing by 6.8 days for each 1 °C increase (Vitasse et al., 2009).

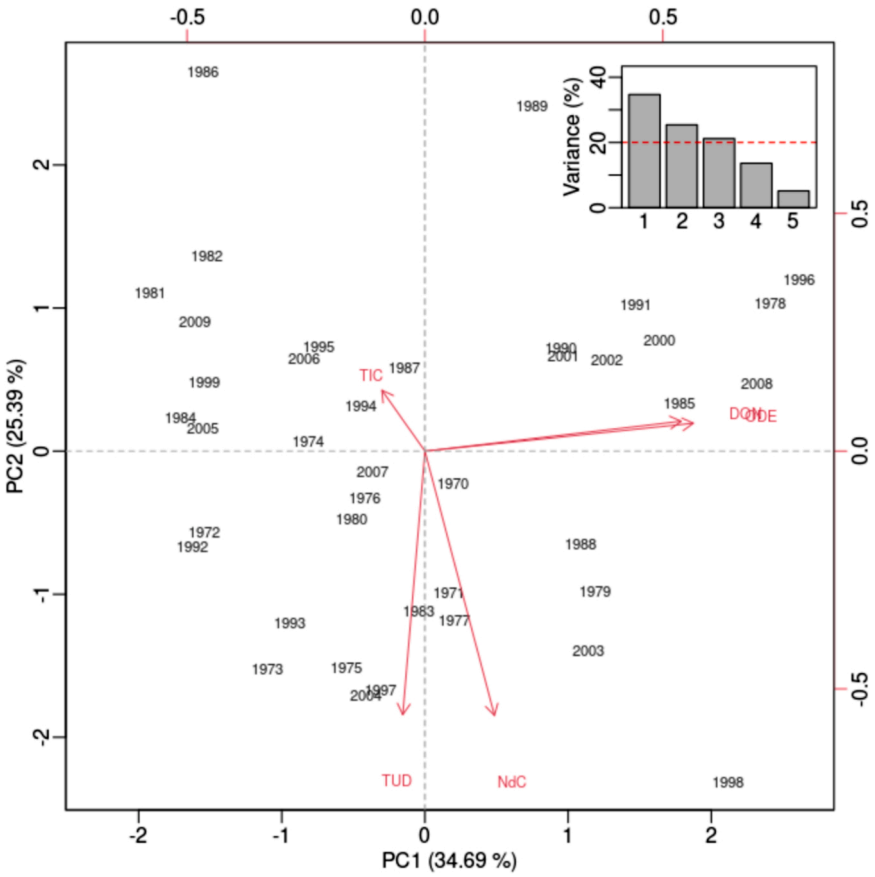

Fig. 3. Chronologies' loadings plotted on the first two principal components (PC1, PC2) of a Principal Component Analysis (PCA). The PCA was calculated on the matrix of the five residual ring-width chronologies, considering the period 1970–2009. The variances explained by the two first principal components are indicated between parentheses and shown in the inset where the dashed line indicates the 20 % variance threshold.

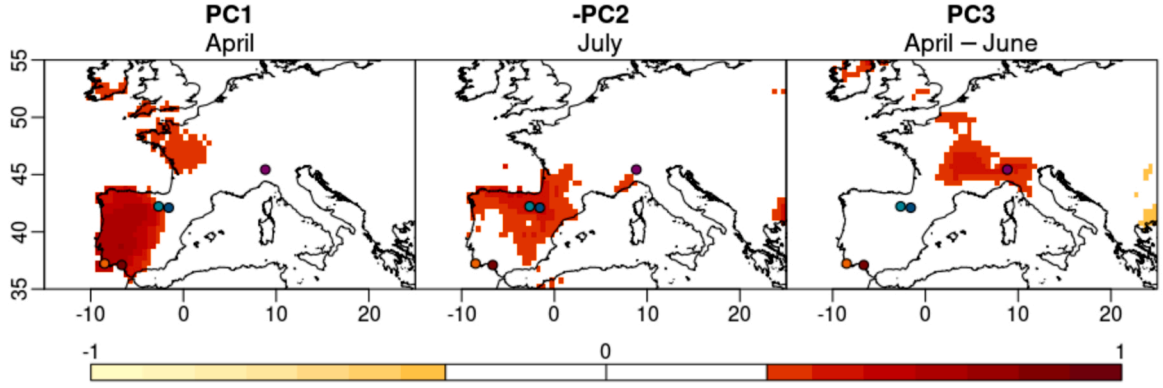

Fig. 4. Spatial correlations between the three first principal components (PCs) and soil water content (SWC) for the period 1970–2009. The sign "−" indicates inverted scores for PC2. Color dots show the five study sites. Correlations which were not significant ($p > 0.05$) have been masked out.

Besides, an earlier spring growth onset in the study region could be driven by the intensive flow of warmer Atlantic air masses linked to changes in the North Atlantic Oscillation phases (Camarero, 2011; Ahas et al., 2002; Hurrell, 1995). This is confirmed by spatial significant positive correlations between late-winter temperature over western Iberia and PC1 scores (Fig. S2). The spatial analysis reveals also that chronologies from closer sites (DON-ODE and NdC-TUD) shared a common signal (Fig. 4) that could be combined to represent the regional hydroclimate variability in Iberian major river basins.

Hydrological year precipitation is crucial to maintain high levels of soil water content during the growing season (Fig. S3), which is the main growth-limiting factor in Mediterranean forests (Pacheco et al., 2016, 2018). The lack of rainfall signal in summer at DON and ODE sites could be explained by low monthly precipitation (< 20 mm) that is not enough to compensate evapotranspiration due to high temperatures (Campelo et al., 2007; González-Muñoz et al., 2015), in contrast to significant correlations with June and July precipitation (> 30 mm) found in NdC and TIC sites. In the wettest (TIC) and coldest (NdC) sites, growth responses to soil water content peak in summer (July and August, respectively), suggesting a late growth onset and peak, which reduces the susceptibility to late spring frosts (Polgar and Primack, 2011).

Table 4
Vaganov-Shashkin parameters estimated for each site and for the best-replicated common period (1970–2009). The last line shows the Pearson correlation coefficients (r) between observed and simulated chronologies which were significant ($p < 0.05$) in the five sites (see Fig. 2). The description of each parameter is given in Table S1.

	Units	DON	ODE	TUD	NdC	TIC	Mean ± SD
T_1	°C	4.91	4.15	8.49	5.03	10.50	6.62 ± 2.74
T_2	°C	13.78	15.58	13.03	14.41	16.42	14.64 ± 1.36
T_3	°C	23.33	22.18	20.5	23.28	21.82	22.24 ± 1.19
T_4	°C	27.65	26.21	25	34.93	26.24	28.01 ± 3.98
M_1	v/v	0.062	0.056	0.075	0.097	0.050	0.07 ± 0.02
M_2	v/v	0.396	0.202	0.330	0.211	0.351	0.30 ± 0.09
M_3	v/v					0.80	
M_4	v/v					0.95	
M0	v/v	0.46	0.35	0.35	0.43	0.37	0.39 ± 0.05
Mmin	v/v					0.065	
Mmax	v/v					0.65	
Pmax	mm	45	45	80	85	70	65.00 ± 19.04
rootD	mm	600	1000	700	700	950	790 ± 174.64
c1	–					0.75	
c2	mm/day					0.13	
c3	$°C^{-1}$					0.19	
Λ	–					0.0005	
tbeg	day					10	
Tbeg	°C	142	140	130	111	141	132.8 ± 13.10
Vcr	–					0.05	
r	–	0.56	0.61	0.49	0.56	0.58	0.56 ± 0.05

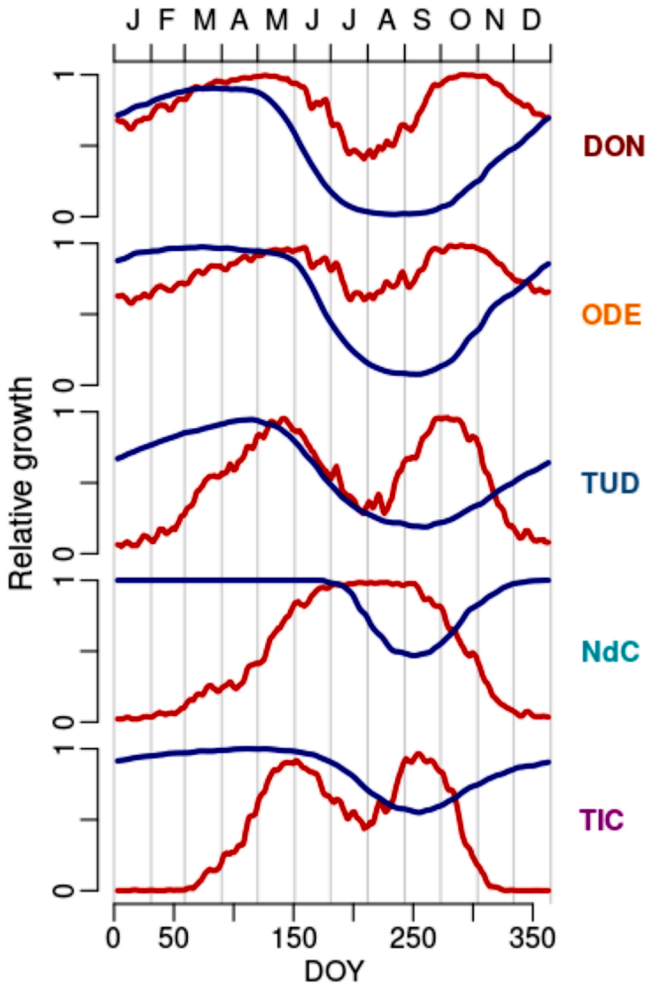

Fig. 5. Mean daily growth response curves (*gT*, *gM*) simulated by the Vaganov-Shashkin model for the period 1970–2009. The growth responses consider temperature (gT, red lines) and soil moisture limitations (gM, blue lines) for the five sites (see Table 1 for sites codes). Note that mean gM values (thick blue lines) decrease from wet-cold (TIC and NdC) to dry-warm sites (ODE, DON and TUD), indicating stronger growth limitations by lower soil moisture.

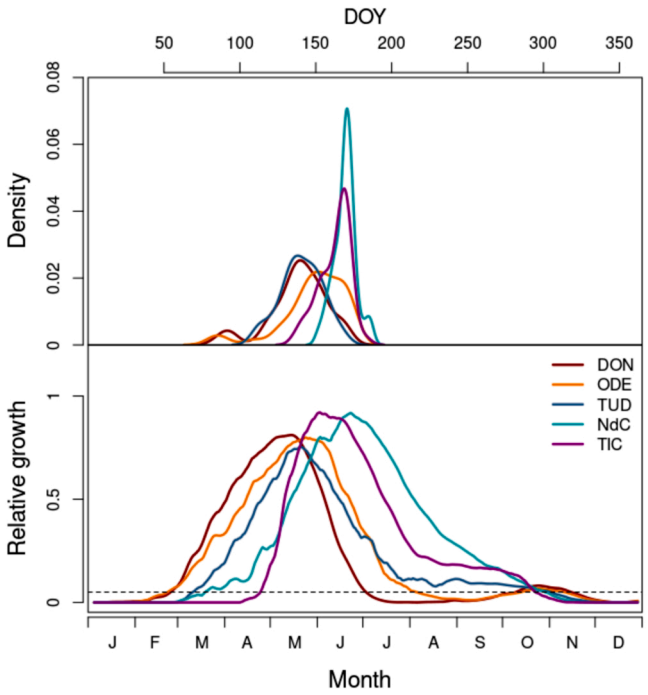

Fig. 6. Density of growth peak (day of the year; DOY) and mean daily growth rates simulated by the Vaganov-Shashkin model.

4.2. *Climate impacts on intra-annual growth patterns*

The intra-annual growth patterns estimated by the VS model matched the relationships observed between ring-width chronologies and soil water content (Fig. 6 and Table 3). Furthermore, at each site the timings of maximal growth estimated by the VS model agree with the timing of highest correlations with soil water content. For instance, at the driest-warmest DON and ODE sites, warmer temperatures in January–February drove an earlier onset of growth and an earlier growth peak around April–May (Fig. 6), which is a safe mechanism to maintain low growth rates during the summer drought (Vieira et al., 2020) without compromising annual growth. In southwestern Iberia, dry soil conditions and high summer temperatures led to reduced or

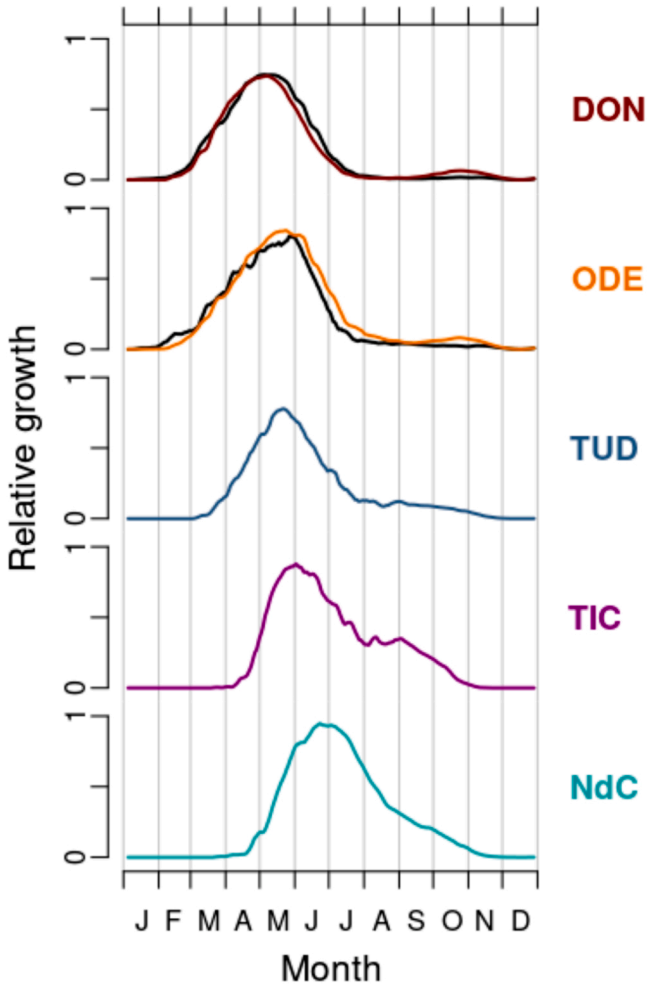

Fig. 7. Daily growth simulated by the Vaganov-Shashkin model for each site. Black lines represent the mean growth simulated for years with an earlier growth stop (before DOY 242), whereas color lines indicate years with longer growing seasons ending after August.

even arrested growth, suggesting that early spring phenological events may be offset by the drought's adverse effect on growing season length (Eilmann et al., 2011). In DON and ODE sites, a second peak of growth could be triggered by early autumn rains, resulting in a bimodal growth pattern. In the wettest TIC site, the high precipitation observed over the growing season led to wood formation being almost decoupled from climate conditions, with the only significant correlation found for temperature (precipitation) in June (July) which corresponded to the period growth peak (Fig. 6). In addition, a tendency towards a late-summer second growth peak was observed, suggesting a potential to grow in response to wet autumn conditions. Some of these results agree with previous findings in ash stands located in a humid continental site in Croatia (Trlin et al., 2021).

4.3. Variable intra-annual growth patterns are contingent on site climate conditions

We showed that intra-annual growth patterns of ash growing under contrasting climatic conditions can be precisely simulated by the VS model. Monthly growth simulations revealed differences in intra-annual growth patterns among sites, as observed for other non-riparian Mediterranean tree species growing in drought-prone areas (Pacheco et al., 2018). Intra-annual growth simulations reveal regional differences in ash growth dynamics that concur with the differences observed in climate-growth associations (Fig. 6 and Table 3). Ash showed three growth patterns: one with a long growing season with a facultative bimodal pattern at the warm DON and ODE sites, a short growing season with a unimodal pattern at the cold NdC and TUD sites, and a short growing season with a slight bimodal pattern in TIC. This species was able to adjust the length of growing season and the timing of growth peak in response to local climatic conditions, which could be particularly advantageous to face increased climate variability (Vieira et al., 2019). The early growth onset in DON and ODE sites is consistent with the variability observed along geographical gradients in which spring phenological events occur earlier at warmer sites (Ahas et al., 2002).

At the driest-warmest DON and ODE sites, simulated growth rates began to decline in late spring and growth resumed after the summer only in years whose late-summer and early-autumn precipitation was sufficient for soil replenishment (Carvalho et al., 2015; Eilmann et al., 2011; Pasho et al., 2012). Trees in DON and ODE sites experience a similar growth reduction period during the dry summer, but while the autumn peak coincides almost perfectly in time, the first peak of high activity in spring and the summer growth fall between peaks was advanced by ~ 2 weeks in the DON site. This advancement could be attributed to an earlier start of water shortage at DON than ODE, which agrees with low growth activity in *Pinus halepensis* Mill. observed during the driest days in summer (Pacheco et al., 2018). The bimodal growth pattern was more evident at the dry-warm DON and ODE sites than in the TUD and NdC cold sites (Fig. 7), where a right-skewed unimodal growth pattern occurred instead (see also Tumajer et al., 2021). According to Pacheco et al. (2018) a more pronounced bimodal growth pattern is observed at coastal sites with high precipitation, mild weather conditions, and long growing seasons. Our findings support a bimodal growth pattern at coastal, mild sites with long growing seasons and a pronounce dry period in summer (Campelo et al., 2021), albeit a slight bimodal pattern was also observed at the wet TIC site, but with no summer interruption.

4.4. Significance of VS model parameters to address growth phenology

We showed that the parameters estimated by the VS model reflect species-specific responses in terms of growth phenology, but also differences of climatic and hydrological conditions across the species' distribution area. The VS model results suggest that this species can adjust the growing season length and intra-annual growth rates to local conditions. In Mediterranean sites, trees can anticipate growth start to ensure that high growth rates are attained before the onset of summer drought, maximizing growth to match favorable conditions (day length, temperature and soil water content). However, anticipating the growing season onset, which permits a longer potential growing season, has an associated cost: maintaining activity during the dry summer. Thus, the longer growing season observed in the Mediterranean region is associated with two main growth peaks interrupted by the summer stop caused by low water availability, which can last for almost 4 months at DON and ODE sites. In these dry-warm sites, a second period of growth could occur in autumn, but only in some favorable years, the so-called facultative bimodal growth pattern (Campelo et al., 2018, 2021). At similar sites, warmer temperatures could extend the growing season by anticipating (delaying) the start (end) of the growing season towards the species specific photoperiod threshold. However, summer drought can trigger an earlier cessation of growth despite favorable conditions in terms of photoperiod and temperature (Lempereur et al., 2017; Vieira et al., 2020). For instance, Ziaco et al. (2018) observed high inter-annual growth variability in *Pinus ponderosa* Douglas ex C. Lawson mainly driven by water availability. In continental sites where mean annual temperature is lower, such NdC and TUD, the growing season tends to be shorter and growth follows a unimodal growth pattern. On the other hand, in the coastal warmer DON and ODE sites, temperature is all-year-round higher than the minimum threshold for tree growth (~ 5 °C) and water availability becomes limiting during summer, leading to the splitting of the potential longer growing season into two main

periods of growth.

The positive growth responses of ash to increased prior-winter temperatures observed in ODE and DON agree with Gomes Marques et al. (2018). Carbon uptake and wood formation can be improved by climate warming (Way and Oren, 2010), but this effect could be counterbalanced by warming-induced evapotranspiration that drives water deficit and triggers reduction in stem radial growth and carbon fixation (Granier et al., 2007). This agrees with previous biogeographical studies that found severe growth reductions in Mediterranean tree species at warmer and drier sites (Sánchez-Salguero and Camarero, 2020). In fact, exceptionally early stem growth cessation (DOY ~ 180) could occur in extremely dry years as forecasted by VS simulations. According to Leuschner et al. (2001), summer drought can enhance fine-root growth thus increasing belowground carbon demands and reducing stem growth, a secondary carbon sink. Additionally, in the warm DON site, phreatic level variations, nutrient availability and soil type could be involved in the reduction of ash growth (Rodríguez-González et al., 2010, 2017), whereas in TUD changes in flood regime could also impact ash performance (Camarero et al., 2021a, 2021b). The expected increase in temperatures predicted by climate models will affect differently growth in ash populations across its distribution area, with carbon uptake decreasing in the driest-warmest sites (e.g., DON and ODE), whereas the opposite could be observed in cold and wet sites (e.g., NdC and TIC).

4.5. Site-conditions' effects on intra-annual growth dynamics

Geographical patterns were detected in growth responses to climate and in intra-annual growth patterns simulated by the VS model (Fig. 6), suggesting that local conditions, such as temperature and soil water content, are the main drivers of growth differences among sites. Under the xeric conditions of DON and ODE sites, the onset of the growing season seems to be driven by temperature and photoperiod (Vieira et al., 2014b), whereas at the cold NdC mountain site cooler temperatures drove a noticeable delay in growth onset and timing of maximal growth rates. Day length and temperature are important environmental cues to determine tree growth phenological events in winter deciduous tree species (Basler and Körner, 2012; Liu et al., 2018). In sites where spring frosts are rare (DON and ODE), bud break could depend on photoperiod and temperature (Marquis et al., 2020).

Phenological responses to climatic warming may reach thresholds once rising temperatures drive phenology towards the species-specific photoperiod threshold (Basler and Körner, 2012). The intra-specific variation in the date of growth onset simulated by the VS model also reflects the spring frost probability experienced at different sites (Marquis et al., 2020). At the two driest DON and ODE sites, monthly radial growth simulations showed a strong growth decrease during the summer in response to soil moisture reduction. Similar results have been found in non-riparian tree species growing under Mediterranean climates such as *Juniperus thurifera* L., *P. halepensis* and *Pinus pinaster* Aiton (Camarero et al., 2010; Campelo et al., 2021; Pasho et al., 2012; Vicente-Serrano et al., 2010; Vieira et al., 2020), but also in riparian tree species (Nadal-Sala et al., 2019). In drought-prone areas, a longer growing season does not always means more tree growth, since ring-width depends more on radial growth rates rather than on growing season length (Li et al., 2021; Ren et al., 2019; Vieira et al., 2020; Zhang et al., 2021; Ziaco et al., 2018). This dependence on growth rates is partially explained by the quiescent summer period imposed by water stress and the existence of two main periods of growth, the so-called bimodal growth pattern (Camarero et al., 2010). In fact, the VS growth simulations suggested that summer drought can trigger a short growing season at the driest sites (Fig. 6). In wet riparian forests of central Europe, droughts can limit radial growth during the driest summer periods, when soil water content is below critical thresholds, and improve water-use efficiency but also can increase productivity due to warmer conditions (Mikac et al., 2018; Kowalska et al., 2020; Schnabel et al., 2022).

4.6. Simulated phenological growth events

The growth onset in the five ash populations was estimated to occur between DOY 50 and 110, while the growth cessation occurs always before DOY 310, suggesting that all populations were not able of extending their growth further into fall (Evans et al., 2016). These estimates agree with our current knowledge on ash species xylem phenology, whose first earlywood vessels start to enlarge before budburst to ensure that are functioning before leaves were fully expanded (Sass-Klaassen et al., 2011; Gričar et al., 2020).

In DON and ODE sites, the potential growing season is longer (from middle February to early November) with a growth peak around May (DOY ~ 140), whereas in the coldest NdC site the growing season is shorter and the timing of growth peak occurs later (DOY ~ 180), reflecting the later growth onset. At low altitude sites, the most influential period for tree growth is around May, when soil moisture is highest (Camarero et al., 2021a, 2021b), whereas at high elevation sites it occurred later (June, July), which is indicative of a shorter growing season due to low temperatures (Huang et al., 2020). The timing of the maximum growth in TIC and NdC sites were close to those reported for conifers in cold environments (Duchesne et al., 2012), which generally synchronize maximum radial growth rates with day length (Rossi et al., 2006), whereas in dry sites the growth peak must be synchronized with soil-water availability.

Differences in growth onset and in the growing season length may explain the differences in the timing of maximal growth. The timing of autumn cessation appears to be less variable in continental sites, possibly because it is primarily determined by photoperiod but enhanced by low temperatures (Atkinson et al., 2013). On the other hand, in coastal mild sites, the timing of growth cessation shows greater variability because along with being triggered by decreasing photoperiod and temperature it can also be anticipated by drought stress (Vieira et al., 2014a).

5. Conclusions

The growth onset in ash trees growing across its southern Europe distribution was driven by temperatures, regardless the soil water content observed at that time. We found that at dry-warm sites, warmer temperatures in spring permit an earlier growth onset, pointing to a lengthening of the growing season. However, a potential longer growing season does not mean higher annual growth rates *per se*. The formation of wider rings is only possible when water availability is not limiting during the season of maximum growth. Our results showed that ash tree growth was mainly driven by soil water content during the growing season. Dry-warm sites trees can show a second growth peak after the summer, but only when autumn water availability improved considerably. Our findings highlight the ability of narrow-leaved ash to adjust its growth to current environmental conditions, which permits this species to reach its potential geographic distribution in the Mediterranean Basin. However, under the ongoing climate warming trees growing under contrasting climatic settings could be affected differently, with trees growing at dry-warm sites being negatively affected by climate warming and increased aridity, whereas trees at wet-cool sites could improved growth due to longer growing seasons. The benefit of a long season may not be fully realized if warmer temperatures reduce soil water content and constrain growth.

Declaration of Competing Interest

The authors declare that they have no known competing financial interests or personal relationships that could have appeared to influence the work reported in this paper.

Data Availability

Data will be made available on request.

Acknowledgments

We are grateful to Antonio Albuquerque for field design, sampling and lab help in Doñana and Odelouca sites and Inês Marques and Rui Rivaes for help during sampling in Odelouca site. We thank the Doñana Biological Reserve and Doñana Biological Station, especially Ricardo Díaz Delgado. We also acknowledge the "Ticino Regional Park" administration for permission and Fulvo Caronni for logistic and field samplings support. This study was partially supported by the BBVA Foundation (SED-IBER project). This work was partially carried out at the R&D Unit Center for Functional Ecology—Science for People and the Planet (CFE), under reference UIDB/04004/2020, and was financed by FCT/MCTES through national funds (PIDDAC). PMRG was supported by Portuguese Foundation for Science and Technology (FCT), through CEEC Individual program Grant no. 2020.03356.CEECIND, and Forest Research Centre is a research unit funded by FCT (UIDB/00239/2020). Field sampling in Odelouca site was supported by RIPFLOW Project (IWRM ERA-net Programme), and in Doñana by the project "Doñana wetland forests as sentinels of global change, funded by the "Programa de Acceso a la Infraestructura Científica y Tecnológica Singular" (ICTS-25-2010), and by project RIFORLONG – "Floodplain forest trajectory restoration assessment using field and remote sensing vegetation indicators", funded by eLTER PLUS (HORIZON 2020), Grant agreement no. 871126. This study was conducted with support of STSM 40285 "Long-term growth and functioning of a major tree species in Mediterranean floodplain forests" to M. Colangelo, funded by COST Action (CA16208) – CONVERGES: Knowledge Conversion for Enhancing Management of European Riparian Ecosystems and Services.

Conflict of Interest

Authors declare no conflict of interest.

Appendix A. Supporting information

Supplementary data associated with this article can be found in the online version at doi:10.1016/j.dendro.2022.126013.

References

Ahas, R., Aasa, A., Menzel, A., Fedotova, V.G., Scheifinger, H., 2002. Changes in European spring phenology. Int. J. Climatol. 22, 1727–1738. https://doi.org/10.1002/joc.818.

Akilli, S., Ulubaş Serçe, Ç., Katircioğlu, Y.Z., Maden, S., 2013. Phytophthora dieback on narrow leaved ash in the black sea region of turkey. For. Pathol. 43, 252–256. https://doi.org/10.1111/efp.12024.

Atkinson, C.J., Brennan, R.M., Jones, H.G., 2013. Declining chilling and its impact on temperate perennial crops. Environ. Exp. Bot. 91, 48–62. https://doi.org/10.1016/j.envexpbot.2013.02.004.

Basler, D., Körner, C., 2012. Photoperiod sensitivity of bud burst in 14 temperate forest tree species. Agric. For. Meteorol. 165, 73–81. https://doi.org/10.1016/j.agrformet.2012.06.001.

Begum, S., Nakaba, S., Yamagishi, Y., Oribe, Y., Funada, R., 2013. Regulation of cambial activity in relation to environmental conditions: understanding the role of temperature in wood formation of trees. Physiol. Plant. 147, 46–54. https://doi.org/10.1111/j.1399-3054.2012.01663.x.

Begum, S., Kudo, K., Rahman, M.H., Nakaba, S., Yamagishi, Y., Nabeshima, E., Nugroho, W.D., Oribe, Y., Kitin, P., Jin, H.-O., Funada, R., 2018. Climate change and the regulation of wood formation in trees by temperature. Trees 32, 3–15. https://doi.org/10.1007/s00468-017-1587-6.

Bunn, A.G., 2008. A dendrochronology program library in R (dplR). Dendrochronologia 26, 115–124. https://doi.org/10.1016/j.dendro.2008.01.002.

Camarero, J.J., 2011. Direct and indirect effects of the North Atlantic Oscillation on tree growth and forest decline in northeastern Spain. In: Vicente-Serrano, S.M., Trigo, R. M. (Eds.), Hydrological, Socioeconomic and Ecological Impacts of the North Atlantic Oscillation in the Mediterranean Region. Advances in Global Change Research, 46. Springer, pp. 129–152. https://doi.org/10.1007/978-94-007-1372-7_10.

Camarero, J.J., Olano, J.M., Parras, A., 2010. Plastic bimodal xylogenesis in conifers from continental Mediterranean climates. New Phytol. 185, 471–480. https://doi.org/10.1111/j.1469-8137.2009.03073.x.

Camarero, J.J., Colangelo, M., Rodríguez-González, P.M., Sánchez-Miranda, Á., Sánchez-Salguero, R., Campelo, F., Rita, A., Ripullone, F., 2021a. Wood anatomy and tree growth covary in riparian ash forests along climatic and ecological gradients. Dendrochronologia 70, 125891. https://doi.org/10.1016/j.dendro.2021.125891.

Camarero, J.J., Rubio-Cuadrado, Á., Gazol, A., 2021b. Climate windows of intra-annual growth and post-drought recovery in Mediterranean trees. Agric. For. Meteorol. 308–309, 108606 https://doi.org/10.1016/j.agrformet.2021.108606.

Campelo, F., Nabais, C., Freitas, H., Gutiérrez, E., 2007. Climatic significance of tree-ring width and intra-annual density fluctuations in *Pinus pinea* from a dry Mediterranean area in Portugal. Ann. . Sci. 64, 229–238. https://doi.org/10.1051/forest:2006107.

Campelo, F., García-González, I., Nabais, C., 2012. detrendeR – a graphical user interface to process and visualize tree-ring data using R. Dendrochronologia 30, 57–60. https://doi.org/10.1016/j.dendro.2011.01.010.

Campelo, F., Gutiérrez, E., Ribas, M., Sánchez-Salguero, R., Nabais, C., Camarero, J.J., 2018. The facultative bimodal growth pattern in *Quercus ilex* – a simple model to predict sub-seasonal and inter-annual growth. Dendrochronologia 49, 77–88. https://doi.org/10.1016/j.dendro.2018.03.001.

Campelo, F., Ribas, M., Gutiérrez, E., 2021. Plastic bimodal growth in a Mediterranean mixed-forest of *Quercus ilex* and *Pinus halepensis*. Dendrochronologia 67, 125836. https://doi.org/10.1016/j.dendro.2021.125836.

Carvalho, A., Nabais, C., Vieira, J., Rossi, S., Campelo, F., 2015. Plastic response of tracheids in *Pinus pinaster* in a water-limited environment: adjusting lumen size instead of wall thickness. PLoS One 10, 1–14. https://doi.org/10.1371/journal.pone.0136305.

Cherubini, P., Gartner, B.L., Tognetti, R., Bräker, O.U., Schoch, W., Innes, J.L., 2003. Identification, measurement and interpretation of tree rings in woody species from mediterranean climates. Biol. Rev. Camb. Philos. Soc. 78, 119–148. https://doi.org/10.1017/S1464793102006000.

Chuine, I., 2010. Why does phenology drive species distribution? Philos. Trans. R. Soc. B Biol. Sci. 365, 3149–3160. https://doi.org/10.1098/rstb.2010.0142.

Chuine, I., Cambon, G., Comtois, P., 2000. Scaling phenology from the local to the regional level: advances from species-specific phenological models. Glob. Chang. Biol. 6, 943–952. https://doi.org/10.1046/j.1365-2486.2000.00368.x.

Cornes, R.C., van der Schrier, G., van den Besselaar, E.J.M., Jones, P.D., 2018. An ensemble version of the E-OBS temperature and precipitation data sets. J. Geophys. Res. Atmos. 123, 9391–9409. https://doi.org/10.1029/2017JD028200.

Duchesne, L., Houle, D., D'Orangeville, L., 2012. Influence of climate on seasonal patterns of stem increment of balsam fir in a boreal forest of Québec, Canada. Agric. For. Meteorol. 162–163, 108–114. https://doi.org/10.1016/j.agrformet.2012.04.016.

Eilmann, B., Zweifel, R., Buchmann, N., Graf Pannatier, E., Rigling, A., 2011. Drought alters timing, quantity, and quality of wood formation in Scots pine. J. Exp. Bot. 62, 2763–2771. https://doi.org/10.1093/jxb/erq443.

Enderle, R., Stenlid, J., Vasaitis, R., 2019. An overview of ash (*Fraxinus* spp.) and the ash dieback disease in Europe. CAB Rev. Perspect. Agric. Vet. Sci. Nutr. Nat. Resour. 14. https://doi.org/10.1079/PAVSNNR201914025.

Etzold, S., Sterck, F., Bose, A.K., Braun, S., Buchmann, N., Eugster, W., Gessler, A., Kahmen, A., Peters, R.L., Vitasse, Y., Walthert, L., Ziemińska, K., Zweifel, R., 2022. Number of growth days and not length of the growth period determines radial stem growth of temperate trees. Ecol. Lett. 25, 427–439. https://doi.org/10.1111/ele.13933.

Evans, L.M., Kaluthota, S., Pearce, D.W., Allan, G.J., Floate, K., Rood, S.B., Whitham, T. G., 2016. Bud phenology and growth are subject to divergent selection across a latitudinal gradient in *Populus angustifolia* and impact adaptation across the distributional range and associated arthropods. Ecol. Evol. 6, 4565–4581. https://doi.org/10.1002/ece3.2222.

Evans, M.N., Reichert, B.K., Kaplan, A., Anchukaitis, K.J.K.J., Vaganov, E.A., Hughes, M. K., Cane, M.A., 2006. A forward modeling approach to paleoclimatic interpretation of tree-ring data. J. Geophys. Res. 111, 1–13. https://doi.org/10.1029/2006JG000166.

Fritts, H.C., 1976. Tree Rings and Climate. Academic Press, London.

Garcia-Forner, N., Vieira, J., Nabais, C., Carvalho, A., Martínez-Vilalta, J., Campelo, F., 2019. Climatic and physiological regulation of the bimodal xylem formation pattern in *Pinus pinaster* saplings. Tree Physiol. 39, 2008–2018. https://doi.org/10.1093/treephys/tpz099.

Gomes Marques, I., Campelo, F., Rivaes, R., Albuquerque, A., Ferreira, M.T., Rodríguez-González, P.M., 2018. Tree rings reveal long-term changes in growth resilience in Southern European riparian forests. Dendrochronologia 52, 167–176. https://doi.org/10.1016/j.dendro.2018.10.009.

González-Muñoz, N., Linares, J.C., Castro-Díez, P., Sass-Klaassen, U., 2015. Contrasting secondary growth and water-use efficiency patterns in native and exotic trees co-occurring in inner Spain riparian forests. For. Syst. 24, 1–10. https://doi.org/10.5424/fs/2015241-06586.

Gordo, O., Sanz, J.J., 2010. Impact of climate change on plant phenology in Mediterranean ecosystems. Glob. Change Biol. 16, 1082–1106. https://doi.org/10.1111/j.1365-2486.2009.02084.x.

Granier, A., Reichstein, M., Bréda, N., Janssens, I.A., Falge, E., Ciais, P., Grünwald, T., Aubinet, M., Berbigier, P., Bernhofer, C., Buchmann, N., Facini, O., Grassi, G., Heinesch, B., Ilvesniemi, H., Keronen, P., Knohl, A., Köstner, B., Lagergren, F., Lindroth, A., Longdoz, B., Loustau, D., Mateus, J., Montagnani, L., Nys, C., Moors, E., Papale, D., Peiffer, M., Pilegaard, K., Pita, G., Pumpanen, J., Rambal, S., Rebmann, C., Rodrigues, A., Seufert, G., Tenhunen, J., Vesala, T., Wang, Q., 2007. Evidence for soil water control on carbon and water dynamics in European forests

during the extremely dry year: 2003. Agric. For. Meteorol. 143, 123–145. https://doi.org/10.1016/j.agrformet.2006.12.004.
Gričar, J., Vedenik, A., Skoberne, G., Hafner, P., Prislan, P., 2020. Timeline of leaf and cambial phenology in relation to development of initial conduits in xylem and phloem in three coexisting sub-Mediterranean deciduous tree species. Forests 11, 1104. https://doi.org/10.3390/f11101104.
Harris, I., Jones, P.D., Osborn, T.J., Lister, D.H., 2014. Updated high-resolution grids of monthly climatic observations – the CRU TS3.10 Dataset. Int. J. Climatol. 34, 623–642. https://doi.org/10.1002/joc.3711.
Hauptman, T., Ogris, N., de Groot, M., Piškur, B., Jurc, D., 2016. Individual resistance of *Fraxinus angustifolia* clones to ash dieback. For. Pathol. 46, 269–280. https://doi.org/10.1111/efp.12253.
Heklau, H., Jetschke, G., Bruelheide, H., Seidler, G., Haider, S., 2019. Species-specific responses of wood growth to flooding and climate in floodplain forests in Central Germany. Iforest - Biogeosci. For. 12, 226–236. https://doi.org/10.3832/ifor2845-012.
Holmes, R.L., 1983. Computer-assisted quality control in tree-ring dating and measurement. Tree-Ring Bull. 43, 69–78.
Huang, J.-G., Ma, Q., Rossi, S., Biondi, F., Deslauriers, A., Fonti, P., Liang, E., Mäkinen, H., Oberhuber, W., Rathgeber, C.B.K.K., Tognetti, R., Treml, V., Yang, B., Zhang, J.-L., Antonucci, S., Bergeron, Y., Camarero, J.J., Campelo, F., Čufar, K., Cuny, H.E., De Luis, M., Giovannelli, A., Gričar, J., Gruber, A., Gryc, V., Güney, A., Guo, X., Huang, W., Jyske, T., Kašpar, J., King, G., Krause, C., Lemay, A., Liu, F., Lombardi, F., Martinez del Castillo, E., Morin, H., Nabais, C., Nöjd, P., Peters, R.L., Prislan, P., Saracino, A., Swidrak, I., Vavrčík, H., Vieira, J., Yu, B., Zhang, S., Zeng, Q., Zhang, Y., Ziaco, E., 2020. Photoperiod and temperature as dominant environmental drivers triggering secondary growth resumption in Northern Hemisphere conifers. Proc. Natl. Acad. Sci. USA 117, 20645–20652. https://doi.org/10.1073/pnas.2007058117.
Hultberg, T., Sandström, J., Felton, A., Öhman, K., Rönnberg, J., Witzell, J., Cleary, M., 2020. Ash dieback risks an extinction cascade. Biol. Conserv. 244, 108516 https://doi.org/10.1016/j.biocon.2020.108516.
Hurrell, J.W., 1995. Decadal trends in the North Atlantic oscillation: regional temperatures and precipitation. Science 269, 676–679. https://doi.org/10.1126/science.269.5224.676.
Janík, D., Adam, D., Hort, L., Král, K., Šamonil, P., Unar, P., Vrška, T., 2016. Patterns of *Fraxinus angustifolia* in an alluvial old-growth forest after declines in flooding events. Eur. J. For. Res 135, 215–228. https://doi.org/10.1007/s10342-015-0925-8.
Köcher, P., Gebauer, T., Horna, V., Leuschner, C., 2009. Leaf water status and stem xylem flux in relation to soil drought in five temperate broad-leaved tree species with contrasting water use strategies. Ann. For. Sci. 66, 101. https://doi.org/10.1051/forest/2008076.
Kowalska, N., Šigut, L., Stojanović, M., Fischer, M., Kyselova, I., Pavelka, M., 2020. Analysis of floodplain forest sensitivity to drought. Philos. Trans. R. Soc. B 375, 20190518. https://doi.org/10.1007/s10584-012-0418-4.
Lelieveld, J., Hadjinicolaou, P., Kostopoulou, E., Chenoweth, J., El Maayar, M., Giannakopoulos, C., Hannides, C., Lange, M.A., Tanarhte, M., Tyrlis, E., Xoplaki, E., 2012. Climate change and impacts in the Eastern Mediterranean and the Middle East. Clim. Change 114, 667–687. https://doi.org/10.1007/s10584-012-0418-4.
Lempereur, M., Limousin, J.-M., Guibal, F., Ourcival, J.M., Rambal, S., Ruffault, J., Mouillot, F., 2017. Recent climate hiatus revealed dual control by temperature and drought on the stem growth of Mediterranean *Quercus ilex*. Glob. Change Biol. 23, 42–55. https://doi.org/10.1111/gcb.13495.
Leuschner, C., Backes, K., Hertel, D., Schipka, F., Schmitt, U., Terborg, O., Runge, M., 2001. Drought responses at leaf, stem and fine root levels of competitive *Fagus sylvatica* L. and *Quercus petraea* (Matt.) Liebl. trees in dry and wet years. For. Ecol. Manag. 149, 33–46. https://doi.org/10.1016/S0378-1127(00)00543-0.
Li, J., Song, F., Jin, Y., Yun, R., Chen, Z., Lyu, Z., Zhao, Y., Cui, D., 2021. Critical temperatures controlling the phenology and radial growth of *Pinus sylvestris* var. *Mongolica* on the southern margin of a cold temperate coniferous forest. Ecol. Indic. 126, 107674 https://doi.org/10.1016/j.ecolind.2021.107674.
Liu, G., Chen, X., Zhang, Q., Lang, W., Delpierre, N., 2018. Antagonistic effects of growing season and autumn temperatures on the timing of leaf coloration in winter deciduous trees. Glob. Change Biol. 24, 3537–3545. https://doi.org/10.1111/gcb.14095.
Marquis, B., Bergeron, Y., Simard, M., Tremblay, F., 2020. Probability of spring frosts, not growing degree-days, drives onset of spruce bud burst in plantations at the boreal-temperate forest ecotone. Front. Plant Sci. 11, 1–19. https://doi.org/10.3389/fpls.2020.01031.
Mikac, S., Žmegač, A., Trlin, D., Paulić, V., Oršanić, M., Anić, I., 2018. Drought-induced shift in tree response to climate in floodplain forests of Southeastern Europe. Sci. Rep. 8, 16495. https://doi.org/10.1038/s41598-018-34875-w.
Mitrakos, K., 1980. A theory for Mediterranean plant life. Acta Oecol.–Oecol. Plant 1, 245–252.
Nadal-Sala, D., Hartig, F., Gracia, C.A., Sabaté, S., 2019. Global warming likely to enhance black locust (*Robinia pseudoacacia* L.) growth in a Mediterranean riparian forest. For. Ecol. Manag. 449, 117448 https://doi.org/10.1016/j.foreco.2019.117448.
Nord, E.A., Lynch, J.P., 2009. Plant phenology: a critical controller of soil resource acquisition. J. Exp. Bot. 60, 1927–1937. https://doi.org/10.1093/jxb/erp018.
Pacheco, A., Camarero, J.J., Carrer, M., 2016. Linking wood anatomy and xylogenesis allows pinpointing of climate and drought influences on growth of coexisting conifers in continental Mediterranean climate. Tree Physiol. 36, 502–512. https://doi.org/10.1093/treephys/tpv125.
Pacheco, A., Camarero, J.J., Ribas, M., Gazol, A., Gutiérrez, E., Carrer, M., Gutierrez, E., Carrer, M., 2018. Disentangling the climate-driven bimodal growth pattern in coastal and continental Mediterranean pine stands. Sci. Total Environ. 615, 1518–1526. https://doi.org/10.1016/j.scitotenv.2017.09.133.
Pasho, E., Camarero, J.J., Vicente-Serrano, S.M., 2012. Climatic impacts and drought control of radial growth and seasonal wood formation in *Pinus halepensis*. Trees 26, 1875–1886. https://doi.org/10.1007/s00468-012-0756-x.
Peñuelas, J., Filella, I., 2001. Phenology: responses to a warming world. Science 294, 793–795. https://doi.org/10.1126/science.1066860.
Polgar, C.A., Primack, R.B., 2011. Leaf-out phenology of temperate woody plants: from trees to ecosystems. New Phytol. 191, 926–941. https://doi.org/10.1111/j.1469-8137.2011.03803.x.
R Development Core Team, 2021. R: A Language and Environment for Statistical Computing. R Foundation for statistical computing, Vienna, Austria.
Ren, P., Ziaco, E., Rossi, S., Biondi, F., Prislan, P., Liang, E., 2019. Growth rate rather than growing season length determines wood biomass in dry environments. Agric. For. Meteorol. 271, 46–53. https://doi.org/10.1016/j.agrformet.2019.02.031.
Roberts, A.M.I., Tansey, C., Smithers, R.J., Phillimore, A.B., 2015. Predicting a change in the order of spring phenology in temperate forests. Glob. Change Biol. 21, 2603–2611. https://doi.org/10.1111/gcb.12896.
Rodríguez-González, P.M., Stella, J.C., Campelo, F., Ferreira, M.T., Albuquerque, A., 2010. Subsidy or stress? Tree structure and growth in wetland forests along a hydrological gradient in Southern Europe. For. Ecol. Manag. 259 (10), 2015–2025. https://doi.org/10.1016/j.foreco.2010.02.012.
Rodríguez-González, P.M., Albuquerque, A., Martínez-Almarza, M., Díaz-Delgado, R., 2017. Long-term monitoring for conservation management: lessons from a case study integrating remote sensing and field approaches in floodplain forests. J. Environ. Manag. 202, 392–402. https://doi.org/10.1016/j.jenvman.2017.01.067.
Rodríguez-González, P.M., Colangelo, M., Sánchez-Miranda, Á., Sánchez-Salguero, R., Campelo, F., Rita, A., Gomes Marques, I., Albuquerque, A., Ripullone, F., Camarero, J.J., 2021. Climate, drought and hydrology drive narrow-leaved ash growth dynamics in southern European riparian forests. For. Ecol. Manag. 490, 119128 https://doi.org/10.1016/j.foreco.2021.119128.
Rossi, S., Deslauriers, A., Anfodillo, T., Morin, H., Saracino, A., Motta, R., Borghetti, M., 2006. Conifers in cold environments synchronize maximum growth rate of tree-ring formation with day length. New Phytol. 170, 301–310. https://doi.org/10.1111/j.1469-8137.2006.01660.x.
Saderi, S., Rathgeber, C.B.K., Rozenberg, P., Fournier, M., 2019. Phenology of wood formation in larch (*Larix decidua* Mill.) trees growing along a 1000-m elevation gradient in the French Southern Alps. Ann. For. Sci. 76, 89. https://doi.org/10.1007/s13595-019-0866-3.
Sánchez-Salguero, R., Camarero, J.J., 2020. Greater sensitivity to hotter droughts underlies juniper dieback and mortality in Mediterranean shrublands. Sci. Total Environ. 721, 137599 https://doi.org/10.1016/j.scitotenv.2020.137599.
Sánchez-Salguero, R., Camarero, J.J., Gutiérrez, E., Gazol, A., Sangüesa-Barreda, G., Moiseev, P., Linares, J.C., 2018a. Climate warming alters age-dependent growth sensitivity to temperature in Eurasian alpine treelines. Forests 9, 1–21. https://doi.org/10.3390/f9110688.
Sánchez-Salguero, R., Camarero, J.J., Rozas, V., Génova, M., Olano, J.M., Arzac, A., Gazol, A., Caminero, L., Tejedor, E., de Luis, M., Linares, J.C., 2018b. Resist, recover or both? Growth plasticity in response to drought is geographically structured and linked to intraspecific variability in *Pinus pinaster*. J. Biogeogr. 45, 1126–1139. https://doi.org/10.1111/jbi.13202.
Sass-Klaassen, U., Sabajo, C.R., den Ouden, J., 2011. Vessel formation in relation to leaf phenology in Pedunculate oak and European ash. Dendrochronologia 29, 171–175. https://doi.org/10.1016/j.dendro.2011.01.002.
Schnabel, F., Purrucker, S., Schmitt, L., Engelmann, R.A., Kahl, A., Richter, R., 2022. Cumulative growth and stress responses to the 2018–2019 drought in a European floodplain forest. Glob. Change Biol. 28, 1870–1883. https://doi.org/10.1111/gcb.16028.
Serrano-Notivoli, R., Martín-Vide, J., Saz, M.A., Longares, L.A., Beguería, S., Sarricolea, P., Meseguer-Ruiz, O., de Luis, M., 2018. Spatio-temporal variability of daily precipitation concentration in Spain based on a high-resolution gridded data set. Int. J. Climatol. 38, e518–e530. https://doi.org/10.1002/joc.5387.
Singer, M.B., Stella, J.C., Dufour, S., Piégay, H., Wilson, R.J.S., Johnstone, L., 2013. Contrasting water-uptake and growth responses to drought in co-occurring riparian tree species. Ecohydrology 6, 402–412. https://doi.org/10.1002/eco.1283.
Skiadaresis, G., Schwarz, J.A., Bauhus, J., 2019. Groundwater extraction in floodplain forests reduces radial growth and increases summer drought sensitivity of pedunculate oak trees (*Quercus robur* L.). Front. For. Glob. Change 2, 267. https://doi.org/10.3389/ffgc.2019.00005.
Stella, J.C., Riddle, J., Piégay, H., Gagnage, M., Trémélo, M.L., 2013. Climate and local geomorphic interactions drive patterns of riparian forest decline along a Mediterranean Basin river. Geomorphology 202, 101–114. https://doi.org/10.1016/j.geomorph.2013.01.013.
Trlin, D., Mikac, S., Žmegač, A., Orešković, M., 2021. Dendrohydrological reconstructions based on tree-ring width (TRW) chronologies of narrow-leaved ash in the Sava river basin (Croatia). Sustainability 13, 1–11. https://doi.org/10.3390/su13042408.
Tumajer, J., Shishov, V.V., Ilyin, V.A., Camarero, J.J., 2021. Intra-annual growth dynamics of Mediterranean pines and junipers determines their climatic adaptability. Agric. For. Meteorol. 311, 108685 https://doi.org/10.1016/j.agrformet.2021.108685.
Vaganov, E.A., Hughes, M.K., Shashkin, A.V., 2006. Growth dynamics of conifer tree rings: images of past and future environments. The Quarterly Review of Biology, Ecological Studies. Springer-Verlag, Berlin/Heidelberg. https://doi.org/10.1007/3-540-31298-6.

Valor, T., Camprodon, J., Buscarini, S., Casals, P., 2020. Drought-induced dieback of riparian black alder as revealed by tree rings and oxygen isotopes. For. Ecol. Manag. 478, 118500 https://doi.org/10.1016/j.foreco.2020.118500.

Vicente-Serrano, S.M., Lasanta, T., Gracia, C., 2010. Aridification determines changes in forest growth in *Pinus halepensis* forests under semiarid Mediterranean climate conditions. Agric. For. Meteorol. 150, 614–628. https://doi.org/10.1016/j.agrformet.2010.02.002.

Vieira, J., Rossi, S., Campelo, F., Freitas, H., Nabais, C., 2014a. Xylogenesis of *Pinus pinaster* under a Mediterranean climate. Ann. For. Sci. 71, 71–80. https://doi.org/10.1007/s13595-013-0341-5.

Vieira, J., Rossi, S., Campelo, F., Nabais, C., 2014b. Are neighboring trees in tune? Wood formation in *Pinus pinaster*. Eur. J. For. Res. 133, 41–50. https://doi.org/10.1007/s10342-013-0734-x.

Vieira, J., Moura, M., Nabais, C., Freitas, H., Campelo, F., 2019. Seasonal adjustment of primary and secondary growth in maritime pine under simulated climatic changes. Ann. For. Sci. 76, 84. https://doi.org/10.1007/s13595-019-0865-4.

Vieira, J., Carvalho, A., Campelo, F., 2020. Tree growth under climate change: evidence from xylogenesis timings and kinetics. Front. Plant Sci. 11, 1–11. https://doi.org/10.3389/fpls.2020.00090.

Vitasse, Y., Delzon, S., Dufrêne, E., Pontailler, J.Y., Louvet, J.M., Kremer, A., Michalet, R., 2009. Leaf phenology sensitivity to temperature in European trees: do within-species populations exhibit similar responses? Agric. For. Meteorol. 149, 735–744. https://doi.org/10.1016/j.agrformet.2008.10.019.

Way, D.A., Oren, R., 2010. Differential responses to changes in growth temperature between trees from different functional groups and biomes: a review and synthesis of data. Tree Physiol. 30, 669–688. https://doi.org/10.1093/treephys/tpq015.

Wigley, T.M.L., Briffa, K.R., Jones, P.D., 1984. On the average value of correlated time series, with applications in dendroclimatology and hydrometeorology. J. Clim. Appl. Meteorol. 23, 201–213. https://doi.org/10.1175/1520-0450(1984)023<0201:OTAVOC>2.0.CO;2.

Zhang, J., Gou, X., Alexander, M.R., Xia, J., Wang, F., Zhang, F., Man, Z., Pederson, N., 2021. Drought limits wood production of *Juniperus przewalskii* even as growing seasons lengthens in a cold and arid environment. Catena 196, 104936. https://doi.org/10.1016/j.catena.2020.104936.

Ziaco, E., Truettner, C., Biondi, F., Bullock, S., 2018. Moisture-driven xylogenesis in *Pinus ponderosa* from a Mojave Desert mountain reveals high phenological plasticity. Plant. Cell Environ. 41, 823–836. https://doi.org/10.1111/pce.13152.